Research Article

SOHAG JOURNAL OF SCIENCES

https://doi.org/10.21608/SJSCI.2022.160309.1031

Expected Risk Minimization and Robust Preventive Inference of Transfer Learning for COVID-19 Diagnosis within Chest X-Rays

Muhammad A.O. Ahmed[1,*], Yasser AbdelSatar[2], and Ibrahim Abbas[2]

[1] *Computer Science Department, Faculty of Computers and Information, Luxor University, Luxor 85951, Egypt.*
[2] *Mathematics Department, Faculty of Science, Sohag University, Sohag 82524, Egypt*
[*] *Email:* mao.khfagy@fci.luxor.edu.eg

Received: 14th September 2022, **Revised:** 25th October 2022, **Accepted:** 27th November 2022.
Published online: 1st January 2023

Abstract: The creation of a treatment strategy and the choice of patient-checking circumstances within many others are supported by early diagnosis of COVID-19 infection. It is possible to detect COVID-19 early on by applying a deep learning method to radiographic medical lab images. Convolutional neural networks (CNN) are used in this study to improve COVID-19 diagnoses using X-ray scans. An automated diagnostic solution that can swiftly deliver accurate diagnostic results is required. CNNs have been found to be efficient at classifying medical images using deep learning techniques. Transfer Learning (TF) is the most reliable research supervised learning method, offering useful analysis to examine many radiographs image samples, and can considerably detect potential and infer preventative detection of COVID-19. Despite its high True Positive, testing healthcare professionals remains a serious risk. Three distinct deep TF and regularization-based architectures were studied on chest X-ray images for the diagnosis of COVID-19. Because these models already include weights trained on the ImageNet database, large training sets are unnecessary. To evaluate the model's performance, 21,165 chest x-ray scan samples were obtained from various sources and identified as COVID-19 data collection from four classes in the Kaggle repository. Average metrics results are collected to get the actual predictions for all classes. Although Saving training time with TF, an advance improvement for performance can be achieved by applying only some parts of the input image with most important segments of the input image are localized. To prove the validity of our approach we use Grad Cam algorithm to find the input image parts with most valuable features for decision making. The localised image region map is udsed to reproduce a lighter version of the image database with only marked as most important image regions. Metrics including precision, F1-Score, confusion matrix, accuracy, sensitivity, specificity, error rate, and error rate have been used to assess the performance of all the TF models., besides false positive (FP), Matthews Correlation Coefficient (MCC), and Kappa performance measures. In terms of performance, the ResNet-50 model outperforms all others with a low error rate of 0.039 and achieves more than a 96% accuracy. The study findings proven the proposed model validity as a computer-aided diagnostics model with a guarantee to supply help for radiologists quickly and accurately.
Keywords: Medical Imaging, COVID-19, X-ray imagery, Xception, ResNet-50, InceptionResNetV3, Adamax.

1. Introduction

COVID-19, a new virus, was discovered in Wuhan, China, at the end of 2019 [1]. The virus has spread across the globe in a few months [2,3]. COVID-19 is a deadly virus that produces severe symptoms in humans, such as cough (76%) and fever (98%) as well as weariness (44%). SARS and respiratory sickness (MERS) are both caused by the COVID-19 virus [4]. Unfortunately, the death rate from COVID-19 is rising every day, which has motivated researchers to put forth endless effort to create a tool that can name all COVID subtypes. This has increased the demand for COVID-19 risk minimization, early identification, and preventive prediction. X-ray image evaluations are also recommended by radiologists for COVID-19 infection-related lung diseases. X-rays have been shown to help COVID-19 patients figure out how the disease is getting worse and how far along it is [5].

According to studies, chest radiographs can supply more reliable findings in the diagnosis of COVID-19 [6,7]. Specialist radiologists evaluate X-ray and CT scans to check for signs of the SARS-CoV-2 infection. However, X-ray image diagnosis may be more difficult than CT image diagnosis, and picture interpretation needs specialized knowledge [8]. The importance of early illness detection and prompt execution of treatment procedures to lower mortality and disease transmission is critical. In pandemic scenarios such as COVID-19, the enormous demand for healthcare services to battle illness may produce bottlenecks. Since COVID-19 is a recently found virus throughout the globe, there is a need for intelligent decision support systems because of a lack of ability in diagnosis, disagreement, and uncertainty about the efficacy of the tests used, and an inadequate number of specialists. According to studies, intelligent decision support systems aid specialists in making more correct decisions when recognizing pneumonia-causing illnesses such as COVID-19.

The high penetration of COVID-19 and the typical features of chest images need automated infection diagnosis and localization. Such deep neural network learning algorithms with an intelligent foundation have shown superior talent in image-related challenges, including in a range of radiological

contexts. Although they need a significant amount of training data and powerful machines, they have a lot of promise for supporting COVID-19 detection. When developing neural network models for image classification [9], the task-specific characteristics of the images in the different classes change. They're based on traditional models that have been fine-tuned for purposes such as COVID-19 diagnosis and classification using X-ray image data. As the symptoms of COVID-19 in X-ray images are not always obvious or readable to the human eye, the computer can aid the healthcare professional in making the diagnosis of COVID-19 owing to its fast speed and objective repeatable judgment. The identification and classification of COVID-19 have been made possible by several computer-aided methods. Deep learning is a strong machine learning method that uses a complicated decision-making process to classify organized or unstructured data [10].

When it refers to characteristics that the human visual system cannot recognize, a well-trained deep neural network can notice and explain this similarity. The suggested model primarily pertains to helping medical experts with the prompt detection and recovery of people infected with COVID-19. The present image classification issue is a challenge that requires supervised learning [11,12]. Supervised learning is a learning technique in which an algorithm is trained on a labelled dataset, which means that the real classes of the samples are already supplied to the model, allowing it to adapt its parameters depending on the training accuracy [13,14]. As a solution to this problem, transfer learning was used to use strategies that had already been trained, a training network, and then to tweak the model for correct results and a quick end.

2. Related works

Deep learning models have been more popular in recent years for screening, diagnosis, and therapy management of a variety of illnesses by extracting distinguishing characteristics from medical images. Several automated models for pathology detection and categorization, segmentation of contaminated zones, and severity monitoring have been implemented in response to the COVID-19 outbreak. Since the finding of COVID-19, so many experimental studies in a variety of fields have been conducted. Particularly in the past two years, the number of studies on the primary diagnosis caused by COVID-19 using CNN-based methods rather than chest radiography has grown. The authors of [15] provided a system in which several CNN models used in ensemble learning were applied using transfer learning. They obtained various accuracy rates by training their ensembles using 16,700 X-ray scans from four publicly available datasets. A study [16] achieved 92.86 % accuracy with the AlexNet model and 94.23 % accuracy with the ResNet18 model in their classification investigation utilizing transfer learning on X-ray images of 1346 healthy and 3883 pneumonia patients. The authors of [17] used three pre-trained models to improve and normalize X-ray images to get a diagnosis accuracy of 90.3% for COVID-19. Deep transfer learning and whole-slide data were utilized in research to diagnose invasive ductal cancer. COVID-Net, a deep network for COVID-19 diagnosis developed in [18], accurately classified instances of COVID-19 with 92.4% accuracy. This paper [19] employed the VGG19, Inception, MobileNetV2, Xception, and ResNetV2 models, with the VGG19 model achieving the highest level of accuracy 93.48% on X-ray and CT scans. Deep learning models trained on these images improved the diagnostic utility of these images by simplifying lung recognition, infection localization, illness detection, and classification. Two deep learning models were used in this work for quick COVID-19 diagnosis. For identifying aberrant slices from CT volumes and illness detection, the first model was constructed with two CNN subnetworks, Inception ResNet v2 and ResNet18. The second model was created as a hybrid of the CNN and the Multilayer Perceptron (MLP) [20]. The MLP was trained for COVID-19 classification using joint feature vectors consisting of 512-dimensional data recovered from the CT image by the CNN and 12 clinical characteristics. When compared to human experts, this model is said to reach higher classification accuracy. Similarly, for COVID-19 management using CT lung images, [21] suggested a two-stage deep learning approach. It forms a lung lesion segmentation network and a lesion map-trained detection network. Using clinical information and lung lesion characteristics generated from lesion maps, this approach offers prognosis analysis. Even though CT imaging tests are highly recommended in the diagnosis of COVID-19, various deep learning models based on X-ray images have recently been described, owing to their quick collection, low cost, and easy imaging mechanism.

The authors [22] supply a public dataset called COVIDx, which has 13,975 X-ray images of 13,870 patients, as well as a deep learning network named COVID-Net, considering the importance of X-ray images in COVID-19. According to reports, this network has a classification accuracy of 93.3 %.

A deep learning network was suggested by the authors of [23] for automating the COVID-19 diagnostic. The performance of their binary-class strategy was near 98%, while the performance of their multi-class strategy was near 87%. Three different modified ultramodern pre-trained models were created for the identification of normal, COVID-19, Lung Opacity (non-COVID-19 lung infection), and viral pneumonia cases. Three separate classification methods were performed on the dataset, including 21,165 X-ray images in this research. The accuracy, Sensitivity, specificity, error rate, precision, F1-Score, confusion matrix, FP, MCC, and Kappa measures were used to assess the models' performance. The model with the best TP was used to create a test application. The results proved that the application worked well in practice and that it may be a helpful decision-making tool for specialists.

The rest of this work is arranged in the following manner: Sect. 2 presents a review of earlier work in the context of this study. The proposed data and the suggested methods are presented in detail in Section 3. Sect. 4 describes the model architecture used for the model and details of its implementation. Sect. 5 has the experimental findings, performance assessments, and comparisons. Section 6 addresses the conclusions, as well as some future work.

3. Material and Methods

3.1. Data Preparation

COVID-19 Radiography Database[1]: A large dataset was created using chest X-ray images. This dataset includes information on COVID-19-positive patients as well as data on

normal individuals and those who have contracted viral pneumonia. The most recent release includes Posterior-to-Anterior (PA) view images of 3616 COVID-19 positives, 10192 normal, 6012 Lung Opacity, and 1345 Viral Pneumonia images. This dataset has received help from the work of 43 distinct papers; the Italian SIRM dataset1, the COVID Chest X-ray Dataset [24], and the chest X-ray image database 2. Sample images from four different classes in the dataset are given in Fig. 1.

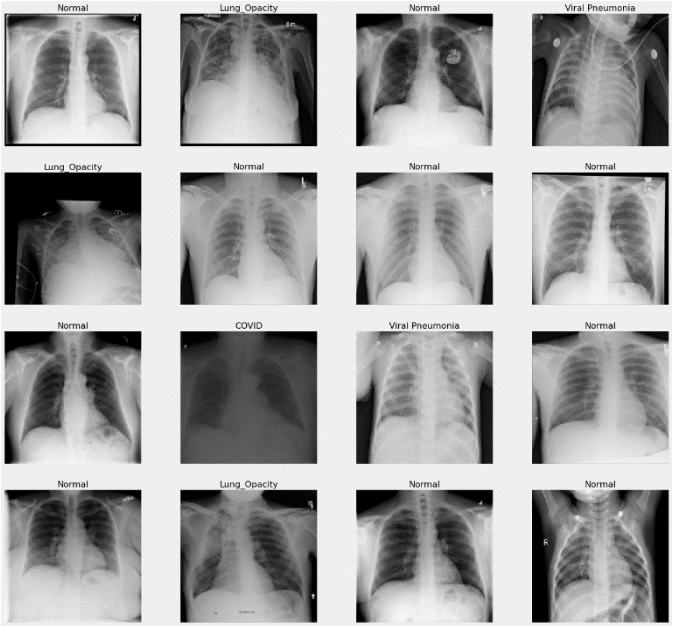

Fig. 1: Cases of chest X-ray images of for classes from Kaggle dataset.

3.2. Pre-processing

Image rescaling and normalization are used in image pre-processing. The COVID-19 radiography image dataset is taken from the well-known Kaggle dataset, which is the actual data recently gathered. Along with photos for typical instances, the collection also contains chest X-ray images for four types of COVID-19 patients. The distribution of the radiography Kaggle dataset is shown in Fig. 2. Using Scikit-train learns to test split module, the dataset was used in the ratio of 90% for training and 10% for testing. Based on the split percent, the data is randomly split between the two sets by a random shuffle process. [25] uses a shuffle process algorithm introduced in [25] which uses a random generator number. Our selection is used in the shuffling algorithm to empirically arrive at the value of 120. The split is also stratified to make sure that a certain number of class samples are in each set.

To address the issue, a thorough comparison of the three pre-trained transfer learning models currently being used is included. The three dels ResNet-50, Xception, and InceptionResNetV3 with hyperparameter tuning technique were performed on this data. This study provides the highest level of precision for X-ray images retrieved from three different databases. Additionally, effectiveness across the database has been examined using the adjusted network architectures used for our research. The next suggestions are proposed by this study:

Applying the infrastructure of three common classification results to detect COVID-19.

(i) Evaluating how these networks perform on X-ray imagery.
(ii) Comparing and analyzing modelling measures.

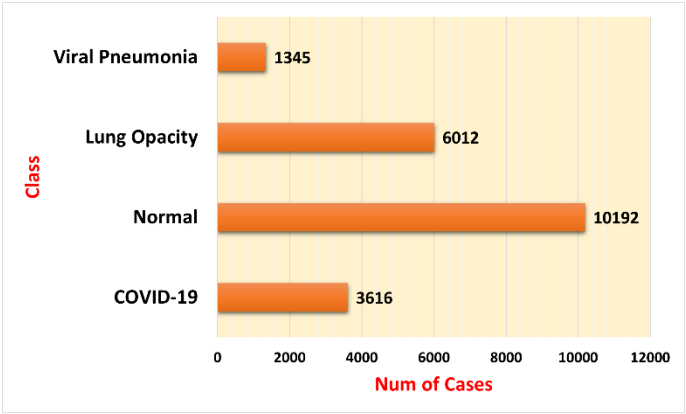

Fig. 2: The latest update version of the proposed COVID-19 Radiography Database.

4. Proposed Model

In this study, we developed a model architecture based on three pre-trained models and a block with three different regularization layers for the generalization process to reduce the over-fitting of the classification of COVID-19 chest X-ray images to normal, Lung Opacity, viral pneumonia, and COVID-19 classes. Additionally, to avoid starting from scratch with training data and save training time, we used a transfer learning technique developed using ImageNet data. Tunable parameters include the number of layers in a CNN model and the number of components in each layer, which change depending on the operation to be done. One of the most important requirements for a neural network model to provide highly accurate results is that it be trained with a large and diverse set of data. Much research employs ultramodern CNN models, which successfully classify nearly 14 million images in the ImageNet dataset and produce high-accuracy results when applied to diverse disciplines. Five of these models, which are often used in academia, were utilized to classify the data in this investigation.

The images were scaled to 224 X 224 for consistency. Following this, ResNet-50, Xception, and InceptionResNetV3 are three different CNN architectures that have been employed. To make use of its features with extensive knowledge and construct the model, a pre-trained model on the ImageNet database is used. Fig. 3 shows the architecture of the suggested CNN model applied to X-ray images. The Adamax optimizer

[1] https://www.sirm.org/category/senza-categoria/covid-19/

[2] https://www.kaggle.com/paultimothymooney/chest-xray-pneumonia

was used to train the final model over 25 epochs, with a 0.001 learning rate. With a 0.99 momentum and 0.001 epsilon, the Batch Normalization layer was introduced to the model. In addition, a dense layer of 64 neurons was added to the model with a rectified linear unit (ReLU) activation function, L2 regularizers with a 0.001 value, and L1 regularizers with a 0.006 value. The output of the base model was flattened because of the top layers of the three models being frozen. A fully connected (FC) layer with a (ReLU) activation function and an added dropout value of 0.4 was also added to the model. For classification, a final layer with SoftMax activation was then applied.

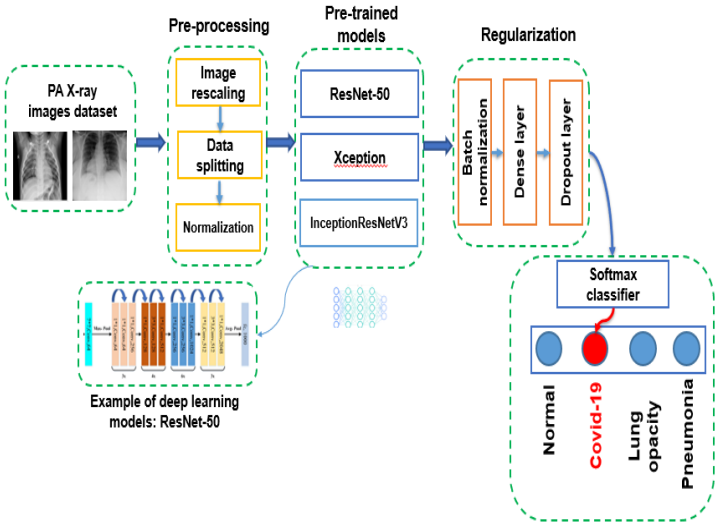

Fig. 3: The general structure of a proposed CNN based TF learning framework with regularization.

4.1. ResNet-50 Network

ResNet, a CNN model, came out on top in the ImageNet competition with an error rate of just 3.5 % [26]. ResNet's structure is based on microarchitecture modules, in contrast to conventional sequential network models. Theoretically, success should rise with the number of layers in a model, but adding more parameters makes training and optimization more challenging. Low activity neurons in the neural network lose their effectiveness during training, and residues appear. Blocks that feed these residues to the following layers are added to build the ResNet. There are multiple ResNet variations that use a varied number of weighted layers. By allowing the gradient to travel across this added shortcut gradient, ResNet lessens the issue of vanishing gradients. If the current layer is not needed, the ResNet model can skip the CNN weight layer thanks to identity mapping. This aids in preventing the over-fitting issue with the ResNet50 training sets of 50 layers.

4.2. Xception Network

The Xception model was presented by Google [27]. The input format for the Xception is a 299x299 RGB image. With 36 convolutional layers to extract features, it has a depth of 126. To reduce the number of parameters, the fully connected layer is swapped out for a global average pooling layer, and the prediction is generated using the SoftMax function. Except for the first and end modules, all the 14 modules composed of the 36 convolutional layers have linear skip connections surrounding them. Entry flow, middle flow, and exit flow are the three sections that form the 36 convolutional layers. The entry flow, the middle flow, which is repeated eight times, and the exit flow are all the steps that the data must initially go through. The middle flow is made up of 8*3=24 convolutional layers, the exit flow is made up of 4 convolutional layers, and the entering flow has 8 convolutional layers. The Xception. model uses depth-wise separable convolution, which can cut down on the overall cost of convolution operations.

4.3. InceptionResNetV3 Network

It has been proven to achieve an accuracy rate of more than 78.1% on the ImageNet dataset, making it a widely used image recognition model. This model is the confluence of many concepts that researchers have developed over time [28]. A deep neural network with 42 layers makes up the Inception-v3. The inception-v3 model's building blocks include convolutions, max-pooling layers, average pooling, dropouts, and FC layers. For example, L1 and L2 regularizes are used to improve the learning process, and weight regularizes are used to encourage the network to support small weights [29]. It can be applied as a general strategy to decrease over-fitting during training and enhance the generalizability of the model. The addition of the batch normalization layer has a fundamental effect on network training, which smooths out the domain of the relevant optimization issue. This makes the gradients more predictable, enabling the adoption of a wider variety of learning rates and accelerating network convergence. Most large network architectures can be generalized using the dropout layer as a generalization technique. Also, it is integrated into the model architecture to overcome the risk of over-fitting.

4.4. Grad Cam

It is important to save either hardware or software resources for a faster and more accurate recognition [30]. The decision of the CNN is made upon a subset of extracted features from all parts of the input image [31]. This image parts varies from information content point of view [32]. There are only parts of the image that the most important attributes are localized. Our hypothesis is that the lugs area represents the most important image parts where the corresponding attributes plays the major rule of the CNN decision. In order to prove our hypothesis, we apply Grad Cam algorithm to highlight the most important image feature's location in blue, meanwhile the less important parts are marked with red. Each CNN supposed to perform diversly because of different architecture. The results of Grad Cam algorithm applied to the three CNN models returned identical results, meaning that all CNN's agreed about where is the most important features are in the input chest image.

5. Experimental Results

a. Evaluation Settings

The Keras framework was used to implement the Resnet-50, Xception, and InceptionResNetV3 design architectures. Keras supplies pre-trained weights from the ImageNet dataset

for these pre-trained networks. Even though the images in the ImageNet dataset within which these networks are trained could not be equivalent to the images obtained for research, they can, however, help by passing new knowledge to better the intended task. Additionally, pre-trained weights reduce the need for a sizable quantity of training data. The Google Colab service was used to execute the programming code. A Tesla P4 GPU was used to speed up processing. All the models were trained using the Adamax Optimizer, and categorical cross-entropy served as the loss function. The batch size was set at training steps, and the epochs were set to 25 for training.

b. Evaluation Parameters

It is essential to measure classification effectiveness in image classification research to scientifically validate the study's findings. Image categorization research have made use of performance assessment measures. These metrics are also utilized in this research to assess the accuracy and reliability of the classification phase. The model's effectiveness is determined by several characteristics, including accuracy, sensitivity, specificity, error rate, precision, F1-Score, confusion matrix, FP, MCC, and Kappa. These are accuracy, specificity, sensitivity, and precision. When the data in the classes is unbalanced, the MCC metric is a beneficial measure. Equations 1–6 show related formulations for each of these measures based on TP, TN, FP, and FN outcomes.

i. $$Accuracy(Acc) = \frac{TN+TP}{TP+FN+FP+TN}. (1)$$

ii. $$Specificity = \frac{TN}{FP+TN}. (2)$$

iii. $$Precision = \frac{TP}{TP+FP}. (3)$$

iv. $$Sensitivity = \frac{TP}{TP+FN}. (4)$$

v. $$F1-Score = 2 \times \frac{Sensitivity \times Precision}{Sensitivity+Precision}. (5)$$

vi. $$MCC = \frac{TP \times TN - FP \times FN}{\sqrt{(TP+FP)+(TP+FN)+(TN+FP)+(TN+FN)}}. (6)$$

The kappa statistic is a chance-corrected measure of agreement instead of correlation. Kappa eq. is described as follows:

$$Kappa = \frac{(\beta - \digamma)}{(\eta - \digamma)}. (7)$$

Where β is the real percentage of agreements among raters, ϝ is the predicted percentage of agreements, and η is the overall count of observations.

c. Evaluation Results

The performance results for the testing data are based on three models, Resnet-50, Xception, and InceptionResNetV3 is shown in Fig. 4. Table 1, 2 present an overview of the findings from these three models. Variety metrics results are collected to get the actual predictions for all classes. Metrics such as accuracy, sensitivity, specificity, error rate, precision, F1-Score, confusion matrix, FP, MCC, and Kappa have been measured to assess the performance of all the models. Three models' accuracy scores show that CNN architectures can reliably diagnose COVID-19 conditions.

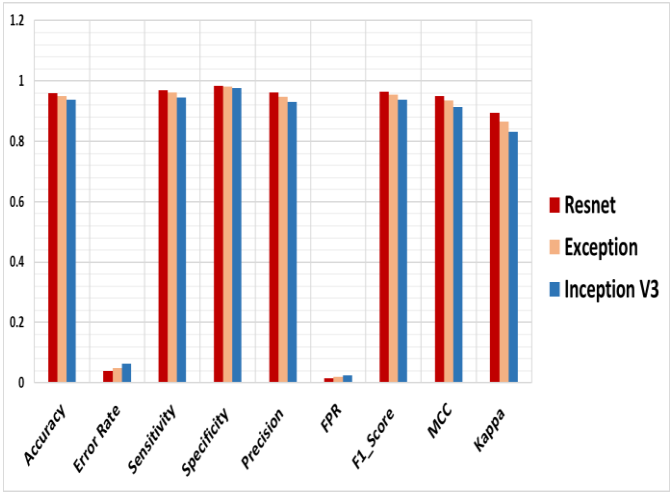

Fig. 4 Analysis of the proposed models based on various evaluation metrics.

From Table 1, ResNet-50 outperforms the other two models with the all-metrics measures as shown in Fig. 4. In the ResNet-50 and Xception models, the TNR, which measures the model's capacity to prevent false alarms, is greater than 93.6 %. However, only ResNet-50 is determined to have excellent error rate and sensitivity, which measures a model's ability to recognize positive cases. Although the Inception ResNet V3 model is relatively like Xception, it can't be regarded as a robust model because of its lower detection rate.

Table 1: Multi-Class Confusion matrix of the proposed model.

Model	Class	TP	FP	FN	TN
ResNet-50	COVID-19	177	6	0	875
	Normal	287	12	23	736
	Lung Opacity	479	21	18	540
	Viral Pneumonia	73	3	1	981
Xception	COVID-19	174	5	3	876
	Normal	283	17	27	731
	Lung Opacity	474	25	23	536
	Viral Pneumonia	74	6	0	978
Inception ResNetV3	COVID-19	166	10	11	871
	Normal	281	23	29	725
	Lung Opacity	471	27	26	534
	Viral Pneumonia	73	7	1	977

Table 2: Present the evaluation metrics tested results for three pre-trained models using X-ray images.

Results Performance	ResNet-50	Xception	Inception ResNetV3
Accuracy	**0.9603**	0.9499	0.9367
Error Rate	**0.0397**	0.0501	0.0633
Sensitivity	**0.969**	0.9624	0.9446
Specificity	**0.9842**	0.9802	0.9757
Precision	**0.9614**	0.9476	0.9315
FP	**0.0158**	0.0198	0.0243
F1-Score	**0.965**	0.9546	0.9377
MCC	**0.9493**	0.9349	0.9134
Kappa	**0.8941**	0.8664	0.8311

According to Fig. 4 and Table 2, the suggested CNN model based on ResNet-50 has a testing accuracy of almost 96% and a specificity rate of 98%. Comparing the suggested model to existing models based on Xception and InceptionResNetV3 networks using different metric findings, it is possible to conclude that the proposed model provides superior performance. In fact, employing many Covid-19 image databases as a training set almost generalizes the suggested model. This means that the proposed model can do very well when tested with data that wasn't used during this training stage.

Another comparison to ensure the approach validity is through a comparison using a single CPU load measured during performing TF using original image database and only using the important image regions which is a relaxation approach to the model objective function during the exhausting search process. A faster way to use TF is guaranteed with CPU load evidence as in Fig. 6, which clarify the model CPU consumption decrease while TF using our approach of input image important regions measurement and localization using Grad Cam algorithm with application to only a single sample from the image database.

Table 3: Evaluating the proposed model to current related research.

Ref	Classes Num.	Accuracy	Sensitivity	Specificity
[19]	3	93.4	98.7	92.8
[33]	2	95	-	-
[16]	3	96.3	-	-
[34]	2	96.2	96.2	96.2
[35]	2	90	-	-
[36]	2	94	-	-
Proposal	**4**	**96**	**96.9**	**98.4**

Finally, Table 3 compares the performance of the proposed model to current studies. This table illustrates that the suggested method outperforms existing methods in terms of the number of types diagnosed and the percentage of analyzed cases.Grad Cam algorithm when applied to the three CNN models returned the images in Fig. 5. Using Grad Cam results, we retrained the TF models using only original image parts which are marked as important, meanwhile dropped the non-important parts to zero. The proposed approach accelerates the training process exponentially besides scoring the same accuracy in test phase.

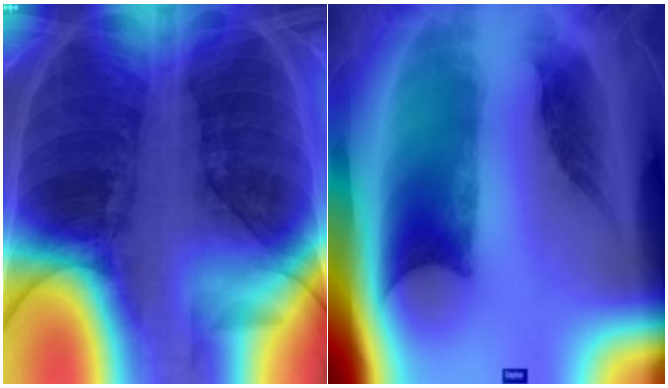

Fig. 5: Grad Cam results, important feature location in the original image is marked in blue, the less importance in other colors grading to red for neglected image regions.

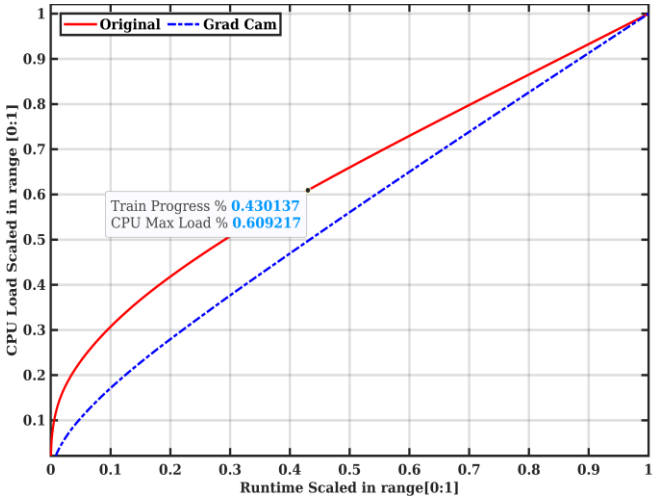

Fig. 6: CPU load consumption using TF without/with important feature localization approach.

6. Conclusion and Future Scope

Using chest imaging with deep learning algorithms provides a reliable and efficient strategy for detecting, diagnosing, and monitoring the progression of COVID-19 conditions. We developed a CNN model pre-trained model based on X-ray images to supply a fast and accurate solution to COVID-19 detection. All networks had been pre-trained, which helped them transfer their prior weights and parameters experience to solve this problem. Fine-tuning and regularization blocks were added to our proposal on chest X-ray imagery for better accuracy in COVID-19 diagnosis. The main idea of adding regularization block layers is to overcome CNN model challenges such as error bias and variance over-

fitting. Different metrics are used to evaluate our models, such as accuracy, error rate, sensitivity, specificity, precision, FP, F1-Score, MCC, and Kappa. Experiments showed that the ResNet-50 pre-trained model has produced the greatest accuracy rate, up to 96%, among the three models. The same scores were obtained using reproduced version of the image database with only marked as important regions via Grad Cam algorithm. Hyothetical significance of both experiment settings proven by the performance metrics results found that the Resnet-50 model is the best model among others. In the future, researchers will evaluate whether a single X-ray scan can find multiple medical problems at once. The current work can be made better by adding CT images as a diagnostic tool for multi-label modeling. As a challenge, there is frequently an enormous daily bulk release of medical image datasets. We need autonomous data techniques to be ready for production.

References

[1] Y. Wang, Q. Sun, S. Yang, R. Pei, G. Xiao, B. Liu, Hum. Ecol. Risk Assess. Int. J., (2022) 1–22.

[2] B. Sekeroglu, I. Ozsahin, Transl. Life Sci. Innov., 25 (2020) 553–565.

[3] M. Pramanik, P. Udmale, P. Bisht, K. Chowdhury, S. Szabo, I. Pal, Int. J. Environ. Health Res., 32 (2022) 723–737.

[4] S.S. Thejeshwar, C. Chokkareddy, K. Eswaran, MedRxiv, (2020).

[5] G.D. Rubin, C.J. Ryerson, L.B. Haramati, N. Sverzellati, J.P. Kanne, S. Raoof, N.W. Schluger, A. Volpi, J.-J. Yim, I.B. Martin, Radiology, 296 (2020) 172–180.

[6] H.X. Guan, Y. Xiong, N.X. Shen, Y.Q. Fan, J.B. Shao, H.J. Li, X.M. Li, D.Y. Hu, W.Z. Zhu, Z.Y. Jin, Radiol Pr., 35 (2020) 1000–0313.

[7] M.-Y. Ng, E.Y. Lee, J. Yang, F. Yang, X. Li, H. Wang, M.M. Lui, C.S.-Y. Lo, B. Leung, P.-L. Khong, Radiol. Cardiothorac. Imaging, 2 (2020) e200034.

[8] B. Antin, J. Kravitz, E. Semanticscholar Org, (2017).

[9] M.A. El-Sayed, Y.A. Estaitia, M.A. Khafagy, Int J Adv Comput Sci ApplIJACSA, 4 (2013).

[10] Y. LeCun, Y. Bengio, G. Hinton, Deep learning, Nature, 521 (2015) 436–444.

[11] D. Ciregan, U. Meier, J. Schmidhuber, Comput. Vis. Pattern Recognit., IEEE, 2012: pp. 3642–3649.

[12] B.A. El-Rahiem, M.A.O. Ahmed, O. Reyad, H.A. El-Rahaman, M. Amin, F.A. El-Samie, Int. Conf. Adv. Mach. Learn. Technol. Appl., Springer, 2019: pp. 23–31.

[13] K. Fukushima, S. Miyake, Neocognitron: Compet. Coop. Neural Nets, Springer, 1982: pp. 267–285.

[14] M. Ahmed, Y. Abdel Satar, I.A. Abbas, HDSNE a New Unsupervised Multiple Image Database Fusion Learning Algorithm with Flexible and Crispy Production of One Database: A Proof Case Study of Lung Infection Diagnose In Chest X-ray Images, 1 (2022).

[15] S. Rajaraman, J. Siegelman, P.O. Alderson, L.S. Folio, L.R. Folio, S.K. Antani, Ieee Access, 8 (2020) 115041–115050.

[16] V. Chouhan, S.K. Singh, A. Khamparia, D. Gupta, P. Tiwari, C. Moreira, R. Damaševičius, V.H.C. De Albuquerque, Appl. Sci., 10 (2020) 559.

[17] D. Keidar, D. Yaron, E. Goldstein, Y. Shachar, A. Blass, L. Charbinsky, I. Aharony, L. Lifshitz, D. Lumelsky, Z. Neeman, Eur. Radiol., 31 (2021) 9654–9663.

[18] Z.Q.L. Linda Wang, A. Wong, COVID-Net, ArXiv Prepr. ArXiv200309871, (2020).

[19] I.D. Apostolopoulos, T.A. Mpesiana, Phys. Eng. Sci. Med., 43 (2020) 635–640.

[20] X. Mei, H.-C. Lee, K. Diao, M. Huang, B. Lin, C. Liu, Z. Xie, Y. Ma, P.M. Robson, M. Chung, Nat. Med., 26 (2020) 1224–1228.

[21] K. Zhang, X. Liu, J. Shen, Z. Li, Y. Sang, X. Wu, Y. Zha, W. Liang, C. Wang, K. Wang, Cell, 181 (2020) 1423-1433. e11.

[22] L. Wang, Z.Q. Lin, A. Wong, Sci. Rep., 10 (2020) 1–12.

[23] T. Ozturk, M. Talo, E.A. Yildirim, U.B. Baloglu, O. Yildirim, U.R. Acharya, Comput. Biol. Med., 121 (2020) 103792.

[24] J.P. Cohen, P. Morrison, L. Dao, K. Roth, T.Q. ArXiv Prepr. ArXiv200611988, (2020).

[25] D.E. Knuth, The art of computer programming, Pearson Education, 1997.

[26] K. He, X. Zhang, S. Ren, J. Sun, Proc. IEEE Conf. Comput. Vis. Pattern Recognit., 2016: pp. 770–778.

[27] F. Chollet, Xception, IEEE Conf. Comput. Vis. Pattern Recognit., 2017: pp. 1251–1258.

[28] C. Szegedy, S. Ioffe, V. Vanhoucke, A.A. Alemi, Thirty-

First AAAI Conf. Artif. Intell., 2017.

[29] S. Alshammari, Y.-X. Wang, D. Ramanan, S. Kong, IEEECVF Conf. Comput. Vis. Pattern Recognit., 2022: pp. 6897–6907.

[30] T.-C. Lin, H.-C. Lee, 4th Int. Conf. Med. Health Inform., 2020: pp. 281–288.

[31] N.I. Papandrianos, A. Feleki, S. Moustakidis, E.I. Papageorgiou, I.D. Apostolopoulos, D.J. Apostolopoulos, Appl. Sci., 12 (2022) 7592.

[32] H. Panwar, P.K. Gupta, M.K. Siddiqui, R. Morales-Menendez, P. Bhardwaj, V. Singh, Chaos Solitons Fractals, 140 (2020) 110190.

[33] O. Stephen, M. Sain, U.J. Maduh, D.-U. Jeong, J. Healthc. Eng., 2019 (2019).

[34] A. Jaiswal, N. Gianchandani, D. Singh, V. Kumar, M. Kaur, J. Biomol. Struct. Dyn., 39 (2021) 5682–5689.

[35] G. Liang, L. Zheng, Comput. Methods Programs Biomed., 187 (2020) 104964.

[36] S. Kumari, E. Ranjith, A. Gujjar, S. Narasimman, H.A.S. Zeelani, Transit. Proc., 2 (2021) 559–565.